AD-A096 686 LOCKHEED MISSILES AND SPACE CO INC PALO ALTO CA PALO --ETC F/G 20/11
DAMAGE CHARACTERISTICS OF AN INFINITE CYLINDRICAL SHELL EXCITED--ETC(U)
MAR 81 T L GEERS, C - YEN N00014-79-C-0619

UNCLASSIFIED LMSC-D686495 NL

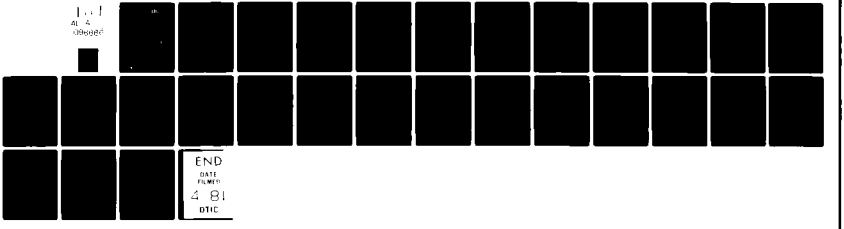

END
DATE FILMED
4 81
DTIC

LEVEL II (1)

MAR 1981

14 LMSC-D686495

DAMAGE CHARACTERISTICS OF AN INFINITE CYLINDRICAL SHELL EXCITED BY A TRANSIENT ACOUSTIC WAVE.

by

T. L. Geers
C.-L. Yen

Sponsored by the Office of Naval Research
Contract N00014-79-C-0619
DUNS 00-912-5535

Approved for Public Release;
Distribution Unlimited

Lockheed Palo Alto Research Laboratory
Palo Alto, California

ABSTRACT

An analytical/computational technique previously developed for determining the geometrically and constitutively nonlinear response of a submerged, infinite cylindrical shell to a transverse, transient acoustic wave is used to study the damage behavior of the shell. Incident waves of rectangular pressure-profile are considered, nonlinear transient response computations are performed, and damage results are described in terms of iso-damage curves based on extensional set strain. Results generated through the use of the doubly asymptotic approximation for treatment of the fluid-structure interaction differ appreciably from their exact counterparts.

TABLE OF CONTENTS

LIST OF TABLES AND FIGURES

Section 1
INTRODUCTION

An analytical/computational technique has recently been developed for determining the geometrically and constitutively nonlinear response of an infinite cylindrical shell to a transverse, transient acoustic wave [1]. The technique involves the use of the structural analyzer DYNAPLAS [2] to treat shell response, and the use of the residual potential formulation [3] to treat the fluid-structure interaction; it has been implemented in the form of a coupled software assembly named RPF-DYNA.

In this study, RPF-DYNA has been used to investigate the damage behavior of a particular shell for incident plane waves of rectangular pressure-profile. The shell exhibits elastic/perfectly plastic material behavior and is characterized by hydrostatic elastic-critical-buckling and elastic-limit pressures that are virtually equal. Because the deformational response of the shell is dominated by extensional motion, damage results are described in terms of iso-damage curves [4] based on extensional set strain.

Iso-damage curves are also constructed for the shell that pertain to the use of the doubly asymptotic approximation (DAA) [5,6] for treatment of the fluid-structure interaction. This approximation, which is the basis for fluid-structure interaction analysis in a number of existing codes [7-12], is asymptotically exact for both low- and high-frequency fluid motions, effecting a smooth transition in the intermediate frequency range. Its computational advantage is that it may be expressed as a matrix ordinary differential equation without requiring discretization of the infinite volume of fluid surrounding the structure.

Section 2
RESPONSE CALCULATIONS

Consider the two-dimensional, plane-strain motions of the submerged, infinite, circular cylindrical shell of Figure 1. The shell is excited by a transient acoustic wave that first contacts the shell at $\theta = \pi$. During the resulting fluid-structure interaction, shell behavior may involve both geometric and constitutive nonlinearity.

2.1 NONDIMENSIONAL RESPONSE EQUATIONS

Following an expansion of the pertinent response variables in circumferential Fourier series, nondimensional response equations for each Fourier harmonic may be derived as [1]

$$\left(\frac{\rho_o}{\rho}\right)\left(\frac{h}{a}\right)\ddot{w}_o + \dot{w} + f_o(v,w) = \dot{\phi}_{Io} + u_{Io} - \frac{1}{2}\phi_{So} + \phi_{Ro}$$

$$\left(\frac{\rho_o}{\rho}\right)\left(\frac{h}{a}\right)\ddot{w}_n + \dot{w}_n + f_{wn}(v,w) = \dot{\phi}_{In} + u_{In} - \frac{1}{2}\phi_{Sn} + \phi_{Rn} + (\dot{\phi}_{Io} + \dot{\phi}_{So})(nv_n + w_n) + \ddot{w}_o w_n,\ n \geq 1 \qquad (1)$$

$$\left(\frac{\rho_o}{\rho}\right)\left(\frac{h}{a}\right)\ddot{v}_n + f_{vn}(v,w) = (\dot{\phi}_{Io} + \dot{\phi}_{So})(v_n + nw_n),\ n \geq 1$$

$$\dot{\phi}_{Sn} + \frac{1}{2}\phi_{Sn} = u_{In} - \dot{w}_n + \phi_{Rn}$$

$$\phi_{Rn} = -r_n * \phi_{Sn}$$

where v_n and w_n are circumferential and radial shell-displacement harmonics, respectively, f_o, f_{vn} and f_{wn} are stiffness-force harmonics computed within DYNAPLAS that involve linear-elastic, geometrically nonlinear and constitutively nonlinear behavior, ϕ_{In} and u_{IN} are fluid-velocity-potential and radial-fluid-particle-

velocity harmonics for the incident-wave field at the shell's wet surface, respectively, ϕ_{Sn} and ϕ_{Rn} are wet-surface scattered-wave-velocity-potential and residual-velocity-potential harmonics, respectively, r_n is a known time-dependent characteristic function [3], and where n is the Fourier index, a dot denotes temporal differentiation and the asterisk denotes temporal convolution. All of the quantities and operations in (1) are nondimensional, normalized in accordance with the convention

$$w_{n.d.} = w/a,\ t_{n.d.} = ct/a,\ \phi_{n.d.} = \phi/ac,\ f_{n.d.} = f/\rho c^2 \qquad (2)$$

For n=0, (1) contains three equations for the three unknowns w_o, ϕ_{So} and ϕ_{Ro}, while for each $n \geq 1$, (1) contains four equations for the four unknowns v_n, w_n, ϕ_{Sn} and ϕ_{Rn}. Here, as in [1], the first three of (1) are solved with the half-step central-difference algorithm, the fourth of (1) is solved with a fourth-order Runge-Kutta scheme, and the last of (1) is solved by trapezoidal integration. This procedure possesses satisfactory accuracy, stability and efficiency characteristics.

2.2 DAMAGE BEHAVIOR

The damage behavior of a particular cylindrical shell with elastic/perfectly plastic material behavior is studied by calculating numerous transient response histories for incident plane waves of rectangular pressure-profile. The shell chosen is the single-layer "compromise shell" of [1], whose inertial, elastic, hydrostatic-elastic-stability, and extensional elastic-limit characteristics match those of a steel sandwich shell, which exhibits in plane-strain fashion the enhanced flexural stiffness properties of stiffened shells. As discussed in [1], the use of the compromise shell is necessitated by the limitation of DYNAPLAS analysis capability to single-layer shells. Table 1 shows the basis of equivalence for the two shells; the only discrepancies pertain to inelastic flexural characteristics, which, as seen below, are of minor significance. Note that the yeld-stress value σ_y is such that the shells' hydrostatic elastic-limit pressure P_0 (whose non-dimensional value is identical to the elastic-limit membrane stress-resultant N_y) exceeds their static-elastic-stability pressure P_0 by 2.4%.

The response variable chosen for damage assessment is circumferential extensional (or membrane) set strain, for two reasons. First, as discussed in [1], the inelastic response of this shell is dominated by extensional motion. Second, extensional shell response almost always reaches its late-time asymptotic limit within five shell-envelopment periods following the passage of the incident wave over the shell; this is in contrast to flexural shell response, which exhibits low-frequency oscillatory behavior for extremely long times. Hence a systematic treatment of flexural set strain requires that each transient response calculation be followed by a dynamic-relaxation calculation involving the introduction of artificial damping to damp out the oscillations. In view of the first reason, the results thus obtained are probably not worth the effort.

Representative inner-fiber and outer-fiber strain response histories are shown in Figure 2. In this case, the magnitude of the incident rectangular wave is five times the static-elastic-stability pressure ($P_I = 5\ P_c$) and the duration of the wave is equal to the shell-envelopment period ($T_I = 2$). For these input parameters, extensional set strain is largest in magnitude at $\theta = 0$. From Figure 2, $|\epsilon^{set}_{ext}|_{max} = 4.8\%$, while $|\epsilon^{set}_{flex}|_{max} \approx 0.15\%$; hence peak flexural strain is only 3% of peak extensional strain in this case.

Highly unrepresentative inner-fiber and outer-fiber strain response histories are shown in Figure 3. In this case, for which $P_I = 1.8\ P_c$ and $T_I = 10$, extensional set strain is largest in magnitude at $\theta = 70°$. From the figure, $|\epsilon^{set}_{ext}|_{max} = 6.0\%$, while $|\epsilon^{set}_{flex}|_{max} \approx 2.5\%$; hence peak flexural strain is about 40% of peak extensional strain in this case.

A more comprehensive picture of the inelastic response results obtained in this study is provided in Table 2. This table summarizes the results obtained in 18 of the more than 50 RPF-DYNA transient response calculations performed. Six quantities are shown for each response calculation, as indicated in the format statement.

Table 2 shows that the set-strain field in the shell is dominated by the $n = 0$ harmonic, with the $n = 1$ and $n = 2$ extensional harmonics making modest

contributions and the higher extensional harmonics contributing very little. Flexural set strain is significant only in a few cases. Maximum extensional set strain usually occurs on the side of the shell that faces away from the incoming wave.

2.3 ISO-DAMAGE CURVES

Calculated values of $|\varepsilon_{ext}^{set}|_{max}$ are shown as circled dots in Figure 4, plotted as functions of magnitude (P_I) and duration (T_I) of the incident rectangular wave. (Recall that P_c is the elastic-critical-buckling pressure for this shell, which is nearly equal to its hydrostatic elastic-limit pressure). The T_I = const. curves that connect the dots permit the accurate estimation of six combinations of P_I and T_I that yield a prescribed value of $|\varepsilon_{ext}^{set}|_{max}$. The selection of five such values then leads to the iso-damage curves of Figure 5.

Figure 5 shows curves of constant $|\varepsilon_{ext}^{set}|_{max}$ plotted in terms of the pressure magnitude and total impulse that completely characterize an incident rectangular wave. Although the curves exhibit the general characteristics of iso-damage curves, i.e., transition from vertical asymptotes for short pulses to horizontal asymptotes for long pulses, they do not possess the simple hyberbolic shapes produced by simple mechanical systems [4].

In Figure 5, each iso-damage curve appears to consist of two damage branches, one for pulses with $T_I \lesssim 3$ and another for pulses with $T_I \gtrsim 3$. The distinctly positive slopes characterizing the high-strain $T_I \lesssim 3$ branches for $T_I \gtrsim 1.5$ produce an unexpected characteristic, viz., that a decrease in pressure magnitude, P_I, for fixed impulse, $P_I\ T_I$, may produce an increase in peak extensional set strain, $|\varepsilon_{ext}^{set}|_{max}$. This is undoubtedly associated with a resonance condition where the shell is especially susceptible to pulses with durations comparable to the shell-envelopment period.

2.4 DOUBLY ASYMPTOTIC APPROXIMATION

As discussed earlier, the doubly asymptotic approximation (DAA) has been extensively used in problems of this type for treatment of the fluid-structure

interaction. Utilization of the DAA in the present problem merely involves taking $\phi_{Rn} = 0$ and replacing the coefficients $\frac{1}{2}$ in (1) by n. As mentioned in [1], the DAA reduces to the plane wave approximation (PWA) for n = 0 in this case.

Extensive DAA-DYNA calculations have been performed for the compromise shell of Table 1. The results of these calculations exhibit dominance of the n = 0 harmonic, as previously seen in the RPF-DYNA results; however, n = 1 strain response emerges in the DAA-DYNA calculations as almost as significant as n = 0 strain response. Contributions to total strain by the higher harmonics, whether extensional or flexural, are generally small in the DAA-DYNA calculations.

Values of $|\epsilon_{ext}^{set}|_{max}$ obtained from the DAA-DYNA calculations are shown as circled dots in Figure 6, plotted in the manner of Figure 4. In contrast to their RPF-DYNA counterparts, these results indicate that peak extensional set strain usually occurs on the side of the shell that faces toward the incoming wave.

The same procedure that produced the iso-damage curves of Figure 5 from the T_I = const. curves of Figure 4 has been used to produce the iso-damage curves of Figure 7 from the T_I = const. curves of Figure 6. Even a cursory comparison of Figures 5 and 7 reveals marked differences between the RPF-DYNA and DAA-DYNA curves. First, and most important, the DAA-DYNA curves for higher-strain values lie well to the right of and above their RPF-DYNA counterparts, which means that use of the DAA may lead to serious underpredictions of damage levels. Second, and less important, the DAA-DYNA curves do not exhibit the resonance behavior observed in the RPF-DYNA curves.

Figs. 5 and 7 demonstrate the general inadequacy of the DAA for treatment of the fluid-structure interaction in the present problem. As mentioned in [1], the reason for this inadequacy is that the DAA reduces to the PWA for n = 0 response, which severely attenuates the rather low-frequency axisymmetric motion characterizing the inelastic response.

To gain insight into possible improvement of the situation just described, response calculations for $P_I = 4\,P_C$, $T_I = 4$ were performed using the cylindrical wave approximation (CWA) [13]. Utilization of this approximation in the present

problem merely involves taking $\phi_{RN} = 0$ in (1). Displacement response histories for n = 0 and n = 1 extensional motion produced by RPF-DYNA, DAA-DYNA and CWA-DYNA are shown in Figure 8. It is seen that the RPF-DYNA histories are bounded by their DAA-DYNA and CWA-DYNA counterparts; unfortunately, the bounds are unacceptably large. Similar histories for n = 1 and n = 2 flexural motion are shown in Figure 9. Here, the RPF-DYNA histories are bounded by their DAA-DYNA and CWA-DYNA counterparts over most of the time span shown; these bounds too are unacceptably large.

Section 3
CONCLUSION

The extensive calculations performed in this study have provided a rather comprehensive picture of the damage behavior of a submerged, infinite cylindrical shell excited by transverse acoustic waves of rectangular pressure profile. This behavior is summarized in the iso-damage curves of Figure 5.

The calculations have also confirmed the failure of the doubly asymptotic approximation as a satisfactory treatment of the fluid-structure interaction for the inelastically excited, infinite cylindrical shell. Such failure was first indicated by a sigle response calculation reported in [1]. A similar calculation based on the cylindrical wave approximation has produced, in this study, slightly better, but still unsatisfactory, results.

The reason for the failure of the doubly-asymptotic approximation is simply that, for the axisymmetric response of the infinite cylindrical shell, it reduces to the plane wave approximation, which is only singly asymptotic. Such reduction does not occur, however, for finite three-dimensional bodies; in fact, the DAA is exact for the n = 0 response of a spherical body.

On the assumption (which has yet to be verified) that the DAA is satisfactory for determination of the inelastic response of a submerged spherical shell to transient acoustic waves, the following question arises: How large may the aspect (length/diameter) ratio become before the DAA fails as a satisfactory treatment of the fluid-structure interaction for inelastic shell-response problems? Seeking the answer to this question is a fitting subject of future work.

Section 4
REFERENCES

1. T. L. Geers and C.-L. Yen, "Inelastic Response of an Infinite Cylindrical Shell to a Transient Acoustic Wave", LMSC-D676214, Lockheed Palo Alto Research Laboratory, Palo Alto, CA, March 1979.

2. W. E. Haisler, J. A. Stricklin and W. A. Von Riesemann, "DYNAPLAS--A Finite Element Program for the Dynamic, Large Deflection, Elastic-Plastic Analysis of Stiffened Shells of Revolution", Rpt. No. TEES-RPT 72-27, Texas A&M University, College Station, TX, December 1972.

3. T. L. Geers, "Excitation of an Elastic Cylindrical Shell by a Transient Acoustic Wave", J. Appl. Mech., 36, 458-469, September 1969.

4. G. R. Abrahamson and H. E. Lindberg, "Peak Load-Impulse Characterization of Critical Pulse Loads in Structural Dynamics", pp 31-53 of Dynamic Response of Structures, G. Herrmann and N. Perrone, eds., Pergamon Press, New York, N.Y., 1972.

5. T. L. Geers, "Residual Potential and Approximate Methods for Three-Dimensional Fluid-Structure Interaction Problems", J. Acoust. Soc. Am., 49, 1505-1510, May 1971.

6. T. L. Geers, "Doubly Asymptotic Approximations for Transient Motions of Submerged Structures", J. Acoust. Soc. Am., 64, 1500-1508, November 1978.

7. G. C. Everstine, "A NASTRAN Implementation of the Doubly Asymptotic Approximation for Underwater Shock Response", NASTRAN: Users Experiences, NASA TM X-3428, 207-228, October 1976.

8. D. Ranlet, F. L. DiMaggio, H. H. Bleich and M. L. Baron, "Elastic Response of Submerged Shells with Internally Attached Structures to Shock Loading", Composites and Structures, 7, 355-364, June 1977.

9. J. A. DeRuntz, T. L. Geers, and C. A. Felippa, "The Underwater Shock Analysis (USA) Code, A Reference Manual", DNA Report 4524F, Defense Nuclear Agency, Washington, D.C., February 1978.

10. J. A. DeRuntz and F. A. Brogan, Underwater Shock Analysis of Nonlinear Structures, A Reference Manual for the USA-STAGS Code", LMSC-D624355, Lockheed Palo Alto Research Laboratory, Palo Alto, CA, February 1978.

11. J. E. Roderick, R. F. Jones, and M. G. Costello, "TRAINS - A Finite Element Computer Program for the Transient, Large Deflection Analysis of Inelastic Structures", Report M-17, David W. Taylor Naval Ship R&D Center, Bethesda, MD, February 1978.

12. R. Atkatsch, M. P. Bieniek and M. L. Baron, "Dynamic Elasto-Plastic Response of Shells in an Acoustic Medium - Theoretical Development for the EPSA Code", Tech. Rpt. No. 24, Weidlinger Assoc., Consulting Engineers, New York, NY, July 1978.

13. J. H. Haywood, "Response of an Elastic Cylindrical Shell to a Pressure Pulse", Quart. J. Mech. and Appl. Math. 11, Pt. 2, 129-141, 1958.

Table 1. SINGLE-LAYER COMPROMISE AND SANDWICH SHELLS *

Single-Layer Shell	Sandwich Shell
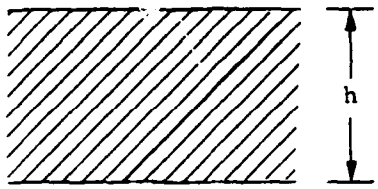	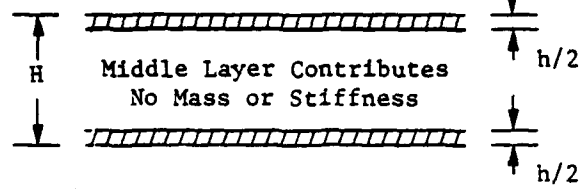
$\frac{h}{a} = 0.1$	$\frac{h}{a} = 0.01, \quad \frac{H}{a} = 0.06266$
$\frac{\rho_o}{\rho} = 0.772, \quad \frac{c_o}{c} = 3.53, \quad \frac{\sigma_y}{\rho c^2} = 0.02188$	$\frac{\rho_o}{\rho} = 7.72, \quad \frac{c_o}{c} = 3.53, \quad \frac{\sigma_y}{\rho c^2} = 0.2188$
Inertial and Elastic Properties	
$\text{"}\rho t\text{"} = \frac{\rho_o h}{\rho a} = 0.0772, \quad \text{"}Et\text{"} = \frac{\rho_o c_o^2 h}{\rho c^2 a} = 0.9620$	$\text{"}\rho t\text{"} = \frac{\rho_o h}{\rho a} = 0.0772, \quad \text{"}Et\text{"} = \frac{\rho_o c_o^2 h}{\rho c^2 a} = 0.9620$
$\text{"}EI\text{"} = \frac{\rho_o c_o^2}{\rho c^2} \cdot \frac{1}{12}\left(\frac{h}{a}\right)^3 = 8.017 \times 10^{-4}$	$\text{"}EI\text{"} = \frac{\rho_o c_o^2}{\rho c^2} \cdot \frac{100}{12}\left(\frac{h}{a}\right)^3 = 8.017 \times 10^{-4}$
Static-Elastic-Stability and Exrensional Elastic-Limit Characteristics	
$P_c = \frac{1}{4}\left(\frac{\rho_o}{\rho}\right)\left(\frac{c_o}{c}\right)^2\left(\frac{h}{a}\right)^3 = 2.405 \times 10^{-3}$	$P_c = 25\left(\frac{\rho_o}{\rho}\right)\left(\frac{c_o}{c}\right)^2\left(\frac{h}{a}\right)^3 = 2.405 \times 10^{-3}$
$N_y = \left(\frac{h}{a}\right)\left(\frac{\sigma_y}{\rho c^2}\right) = 2.462 \times 10^{-3}$ **	$N_y = \left(\frac{h}{a}\right)\left(\frac{\sigma_y}{\rho c^2}\right) = 2.462 \times 10^{-3}$ **
Inelastic Flexural Characteristics	
$M_y = 4.103 \times 10^{-5}$	Yield Moment	$M_y = 6.549 \times 10^{-5}$
$K_y = 0.05118$	Yield Curvature	$K_y = 0.08170$
$M_u = 6.155 \times 10^{-5}$	Ultimate Moment	$M_u = 7.099 \times 10^{-5}$

* See Figure 1 for parameter definitions

** von Mises yield condition with $\nu = 0.3$

Table 2. RPF-DYNA RUNS: SET STRAIN SUMMARY

Format

Maximum Extensional Set Strain Magnitude, $|\epsilon^{set}_{ext}|_{max}$ $\hat{P}_I = P_I/P_c$
Circumferential Location Where Maximum Occurs
Percentage Contribution of n=0 Set Strain to $|\epsilon^{set}_{ext}|_{max}$
Percentage Contribution of n=1 Extensional Set Strain to $|\epsilon^{set}_{ext}|_{max}$
Percentage Contribution of n=2 Extensional Set Strain to $|\epsilon^{set}_{ext}|_{max}$
Approximate Ratio of $|\epsilon^{set}_{flex}|_{max}$ to $|\epsilon^{set}_{ext}|_{max}$

$T_I = \frac{1}{2}$, $\hat{P}_I = 12$	$T_I = \frac{1}{2}$, $\hat{P}_I = 20$	$P_I = \frac{1}{2}$, $\hat{P}_I = 28$
1.823%	5.659%	11.39%
120°	0°	0°
78%	66%	61%
11%	9%	19%
12%	16%	15%
0.06	0.02	0.00
$T_I = 1$, $\hat{P}_I = 3.6$	$T_I = 1$, $\hat{P}_I = 12$	$T_I = 1$, $\hat{P}_I = 18$
1.089%	6.159%	12.40%
0°	0°	70°
41%	78%	87%
16%	10%	5%
20%	9%	7%
0.15	0.01	0.27
$T_I = 2$, $\hat{P}_I = 3$	$T_I = 2$, $\hat{P}_I = 5$	$T_I = 2$, $\hat{P}_I = 9$
1.861%	4.801%	12.09%
0°	0°	0°
55%	63%	80%
24%	14%	18%
12%	13%	0%
0.06	0.03	0.06
$T_I = 4$, $\hat{P}_I = 1.8$	$T_I = 4$, $\hat{P}_I = 3.6$	$T_I = 4$, $\hat{P}_I = 4.2$
1.388%	8.305%	11.09%
60°	0°	0°
69%	64%	66%
7%	23%	23%
8%	10%	9%
0.07	0.02	0.01
$T_I = 6$, $\hat{P}_I = 1.7$	$T_I = 6$, $\hat{P}_I = 2.2$	$T_I = 6$, $\hat{P}_I = 3$
1.890%	4.730%	11.09%
60°	50°	0°
89%	73%	66%
0%	20%	27%
5%	2%	7%
0.04	0.08	0.00
$T_I = 10$, $\hat{P}_I = 1.2$	$T_I = 10$, $\hat{P}_I = 1.8$	$T_I = 10$, $\hat{P}_I = 2.2$
1.182%	5.972%	12.41%
180°	70°	40°
83%	89%	78%
11%	3%	20%
5%	8%	2%
0.10	0.42	0.41

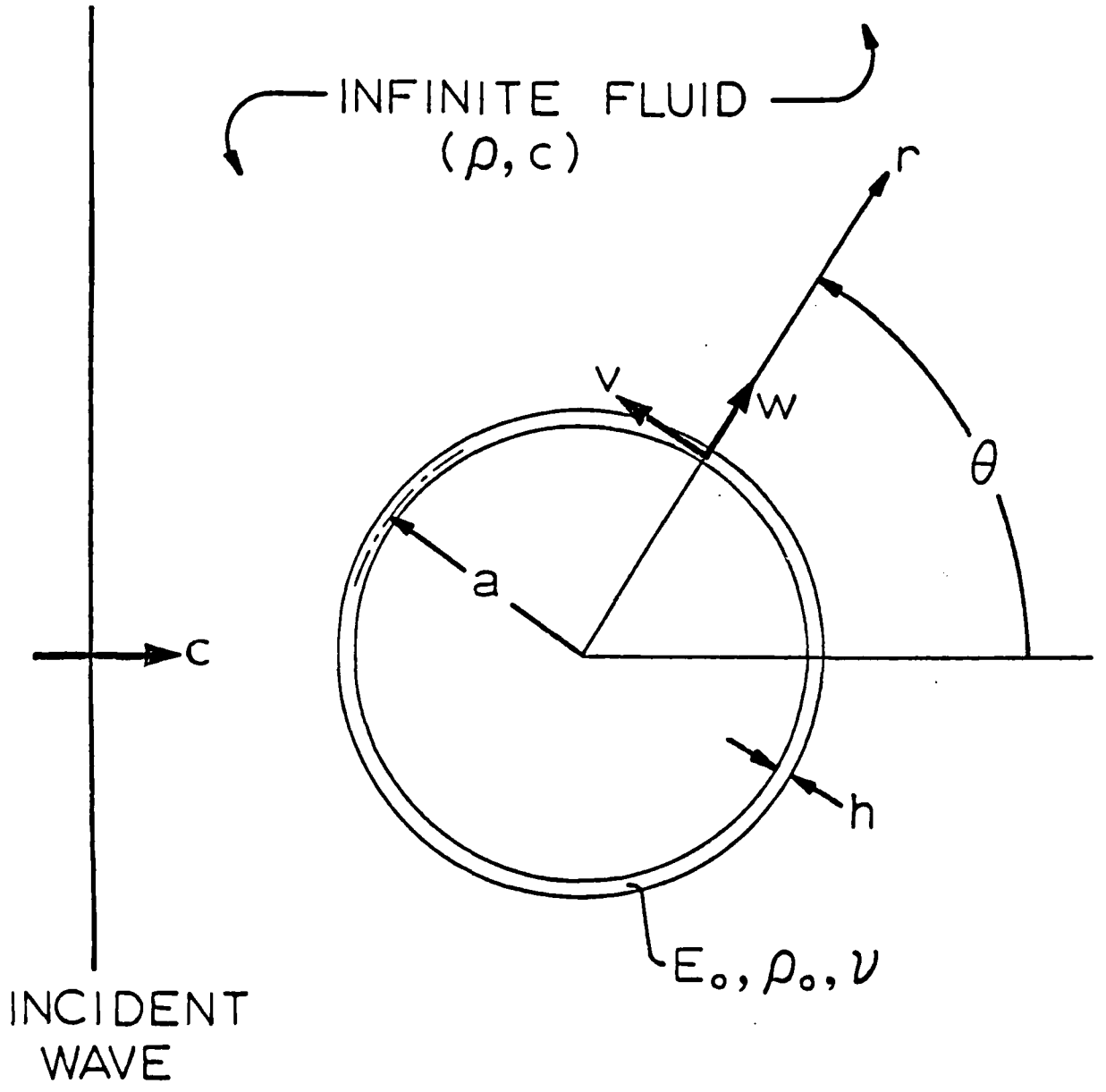

Figure 1. Geometry of Problem

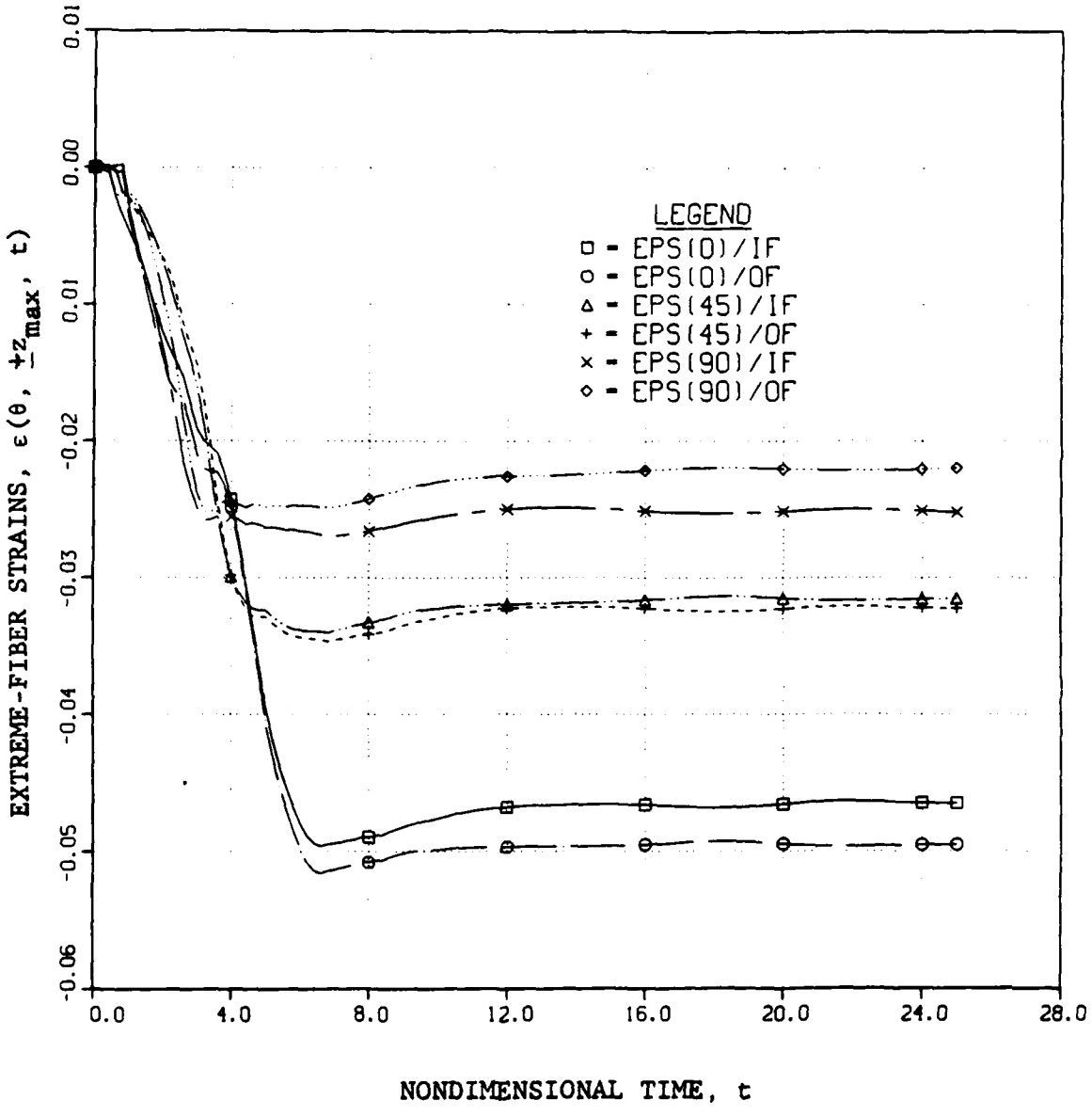

Figure 2 Representative RPF-DYNA Strain Response of Compromise Shell (IF denotes inner fiber; OF denotes outer fiber; $P_I = 4P_c \approx 4P_o$, $T_I = 4$)

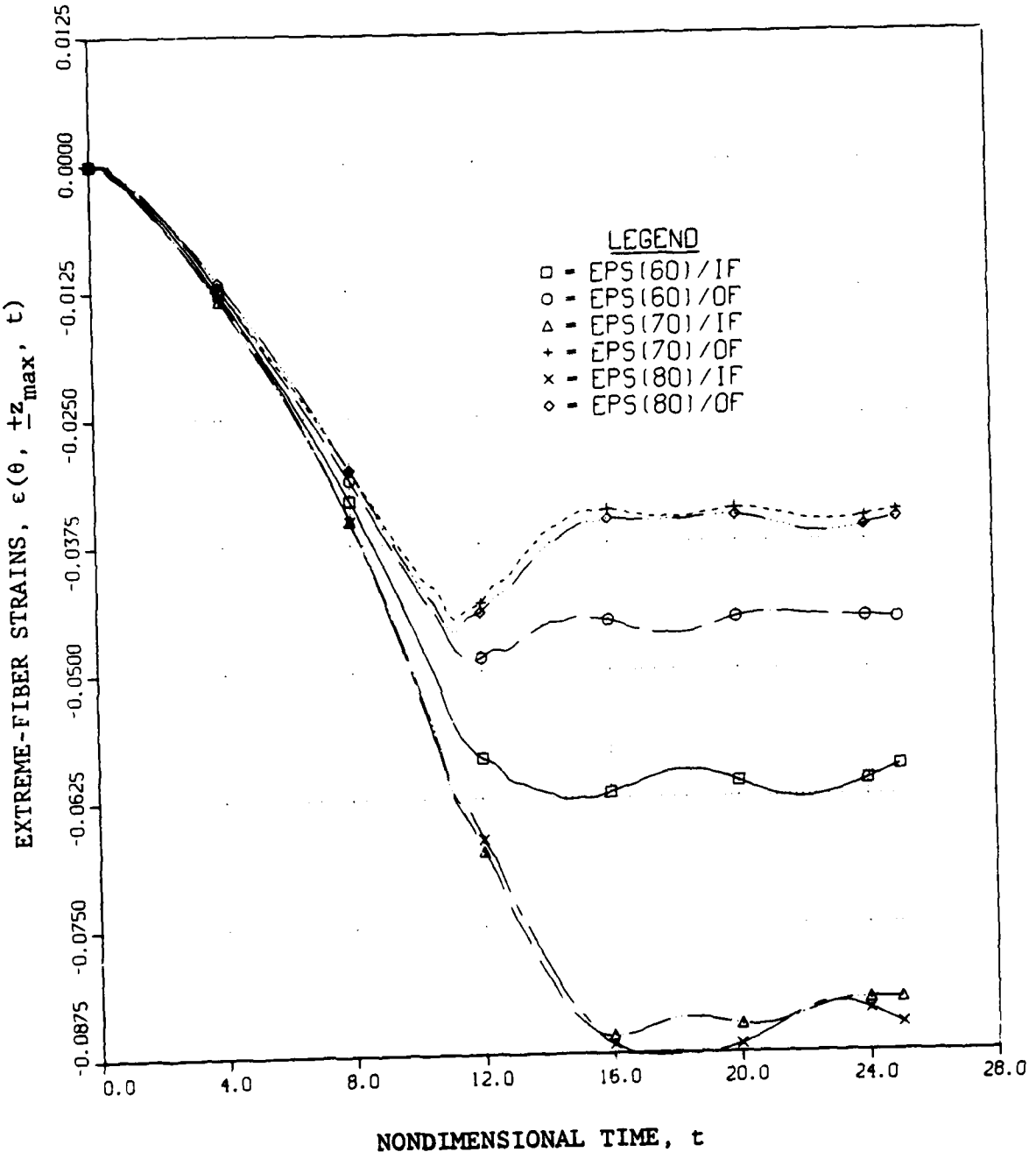

Figure 3 Unrepresentative RPF-DYNA Strain Response of Compromise Shell (IF denotes inner fiber; OF denotes outer fiber; $P_I = 4P_c \approx 4P_o$, $T_I = 4$)

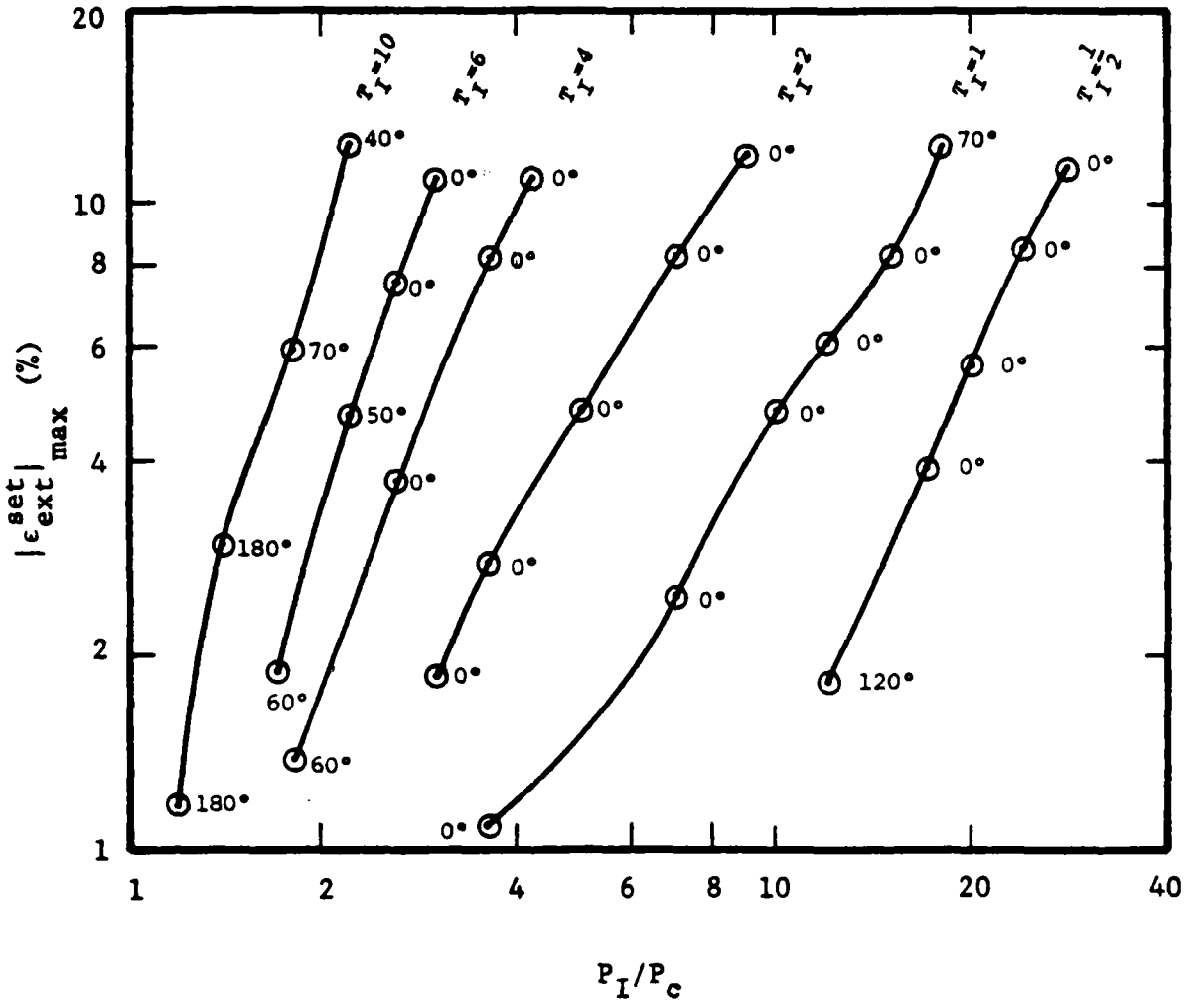

Figure 4 Maximum Extensional Set-Strain Magnitudes as Calculated by RPF-DYNA (angles indicate the locations at which the maxima are reached)

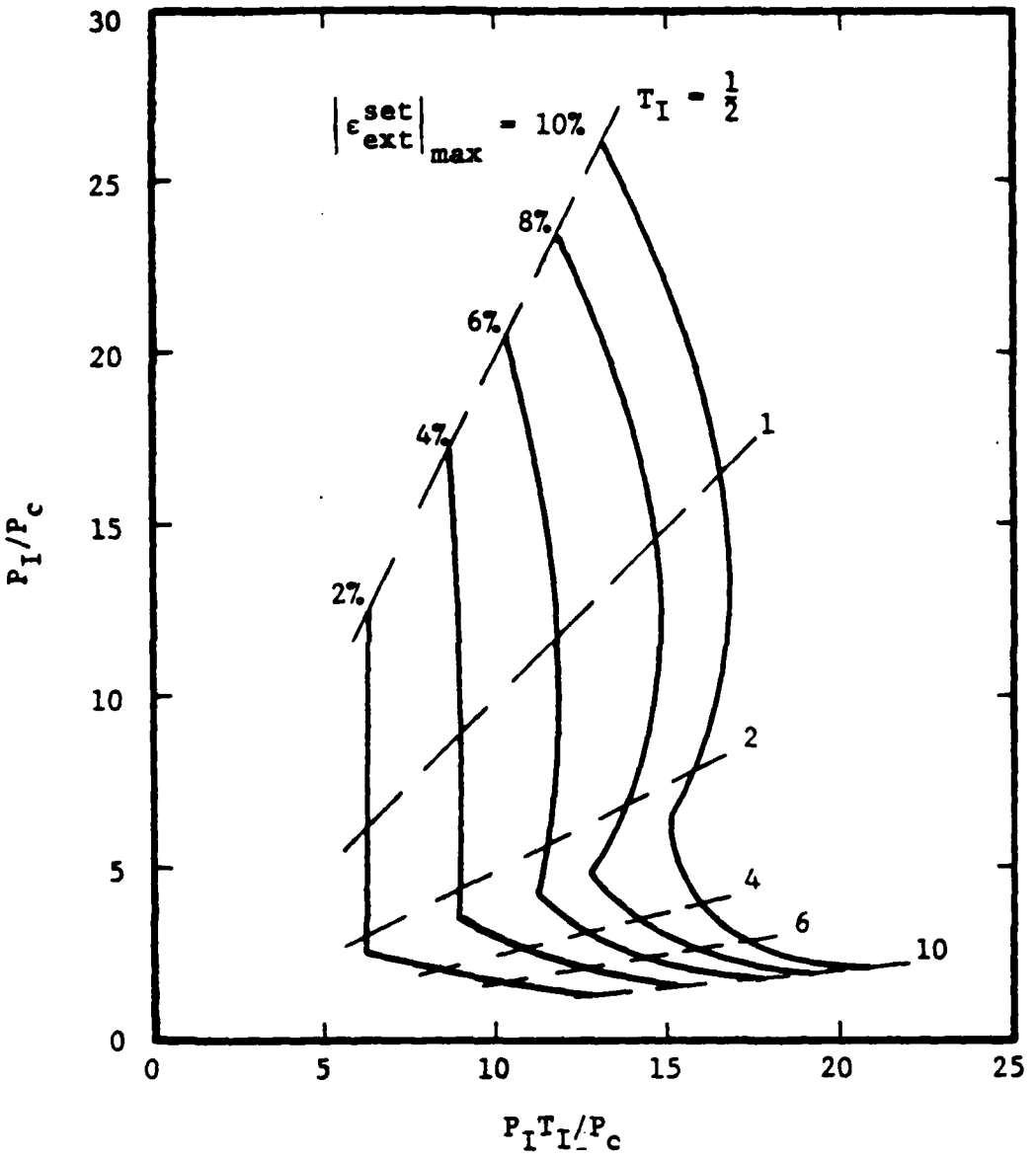

Figure 5 RPF Iso-Damage Curves from the Data of Figure 4

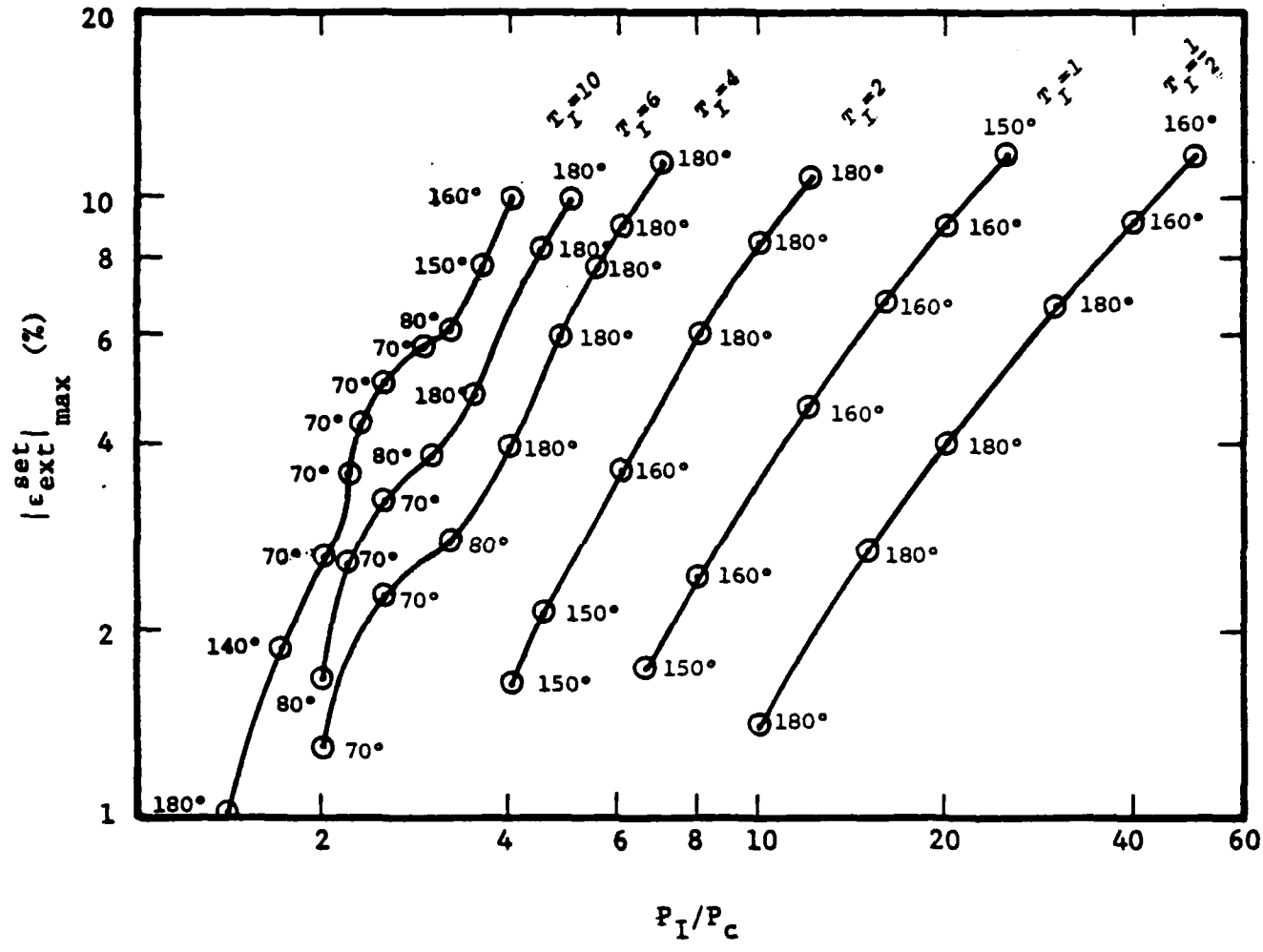

Figure 6 Maximum Extensional Set-Strain Magnitudes as Calculated by DAA-DYNA (angles indicate the locations at which the maxima are reached)

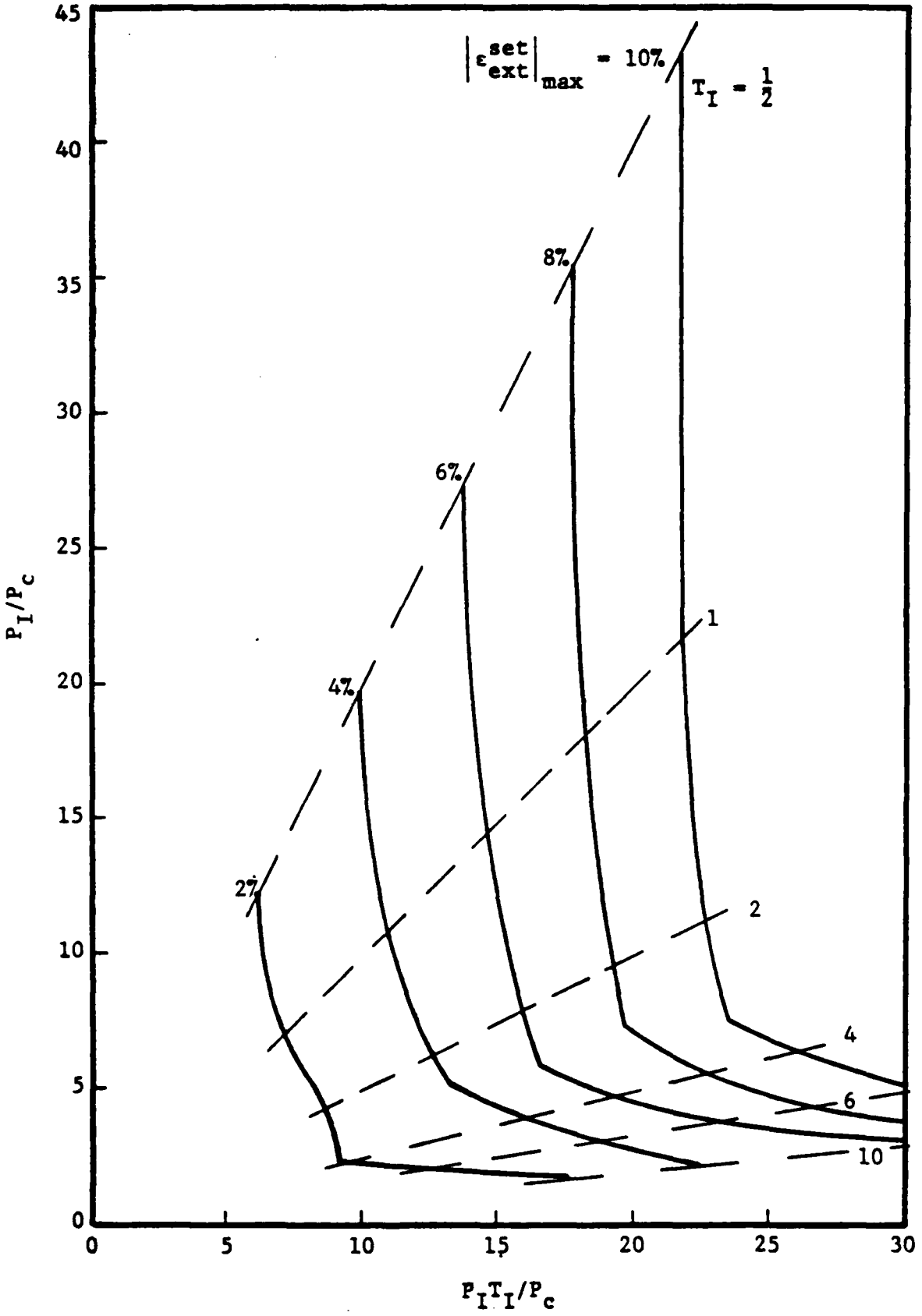

Figure 7 DAA Iso-Damage Curves from the Data of Figure 6

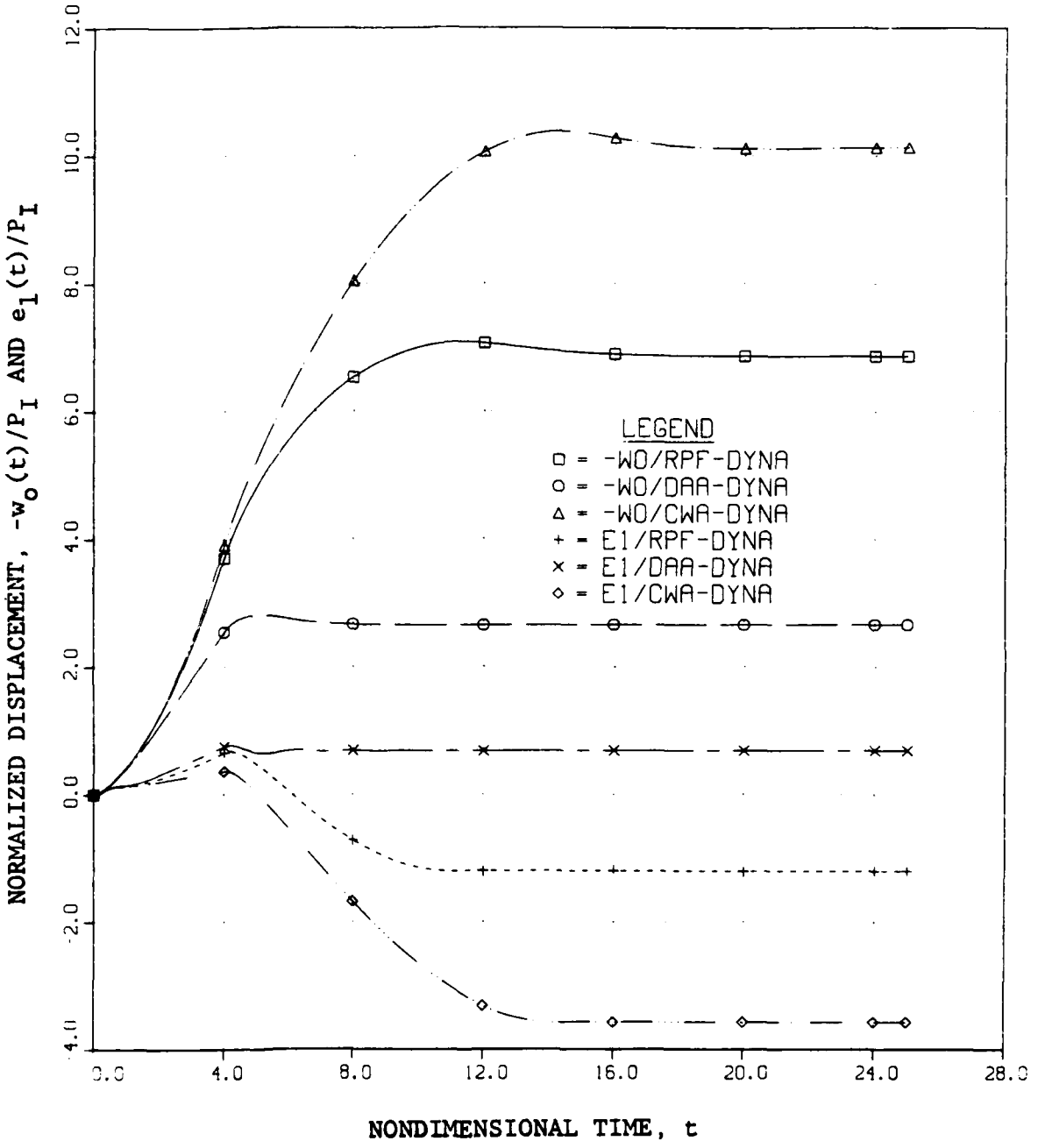

Figure 8 n=0 and n=1 Extensional Displacement Response of Compromise Shell as Computed with RPF-DYNA, DAA-DYNA and CWA-DYNA ($P_I = 4P_c \approx 4P_o$, $T_I = 4$)

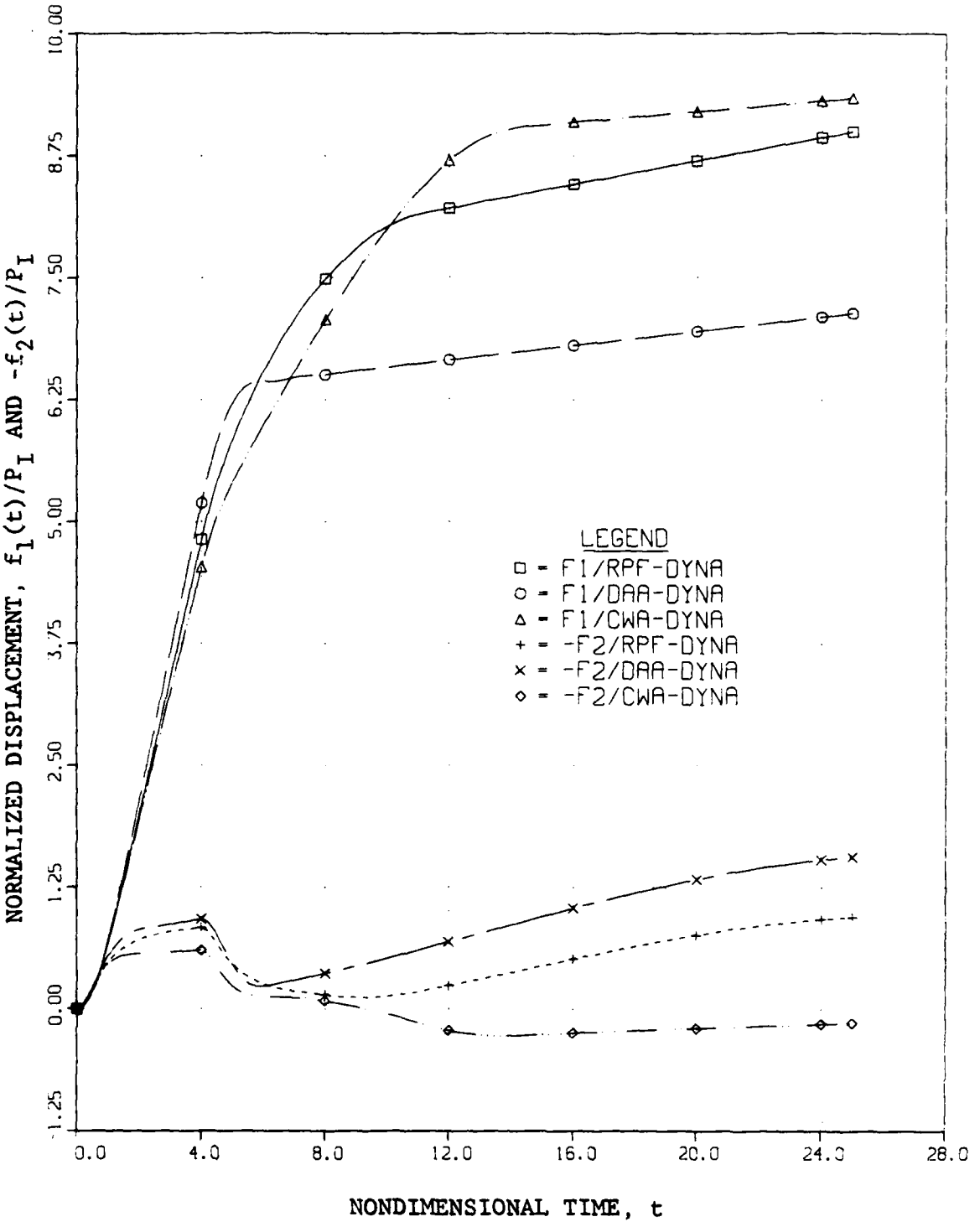

Figure 9 n=1 and n=2 Flexural Displacement Response of Compromise Shell as Computed with RPF-DYNA, DAA-DYNA and CWA-DYNA ($P_I = 4P_c \approx 4P_o$, $T_I = 4$)

DISTRIBUTION

Assistant to the Secretary of Defense
Atomic Energy
Washington, DC 20301
Attn: Executive Assistant

Director
Defense Advanced Research Project Agency
1400 Wilson Blvd.
Arlington, VA 22209
Attn: TIO

Defense Documentation Center
Cameron Station
Alexandria, VA 22314
Attn: DD

Director
Defense Intelligence Agency
Washington, DC 20301
Attn: RDS-3A (Technical Library)
DT-2
DT-1C
DB-4C

Director
Defense Nuclear Agency
Washington, DC 20305
Attn: DDST
TITL
SPSS

Commander
Field Command
Defense Nuclear Agency
Kirtland Air Force Base
Albuquerque, NM 87115

Chief
Field Command
Defense Nuclear Agency
Livermore Division
P.O. Box 808, L-317
Livermore, CA 94550
Attn: FCPRL

Director
Interservice Nuclear Weapons School
Kirtland Air Force Base
Albuquerque, NM 87115
Attn: TTV

Director
Joint Strategic Target Planning Staff
Offutt Air Force Base
Omaha, NB 68113
Attn: NRI-STINFO Library
JLTW/Thompson

Under Secretary of Defense for
Research and Engineering
Department of Defense
Washington, DC 20301
Attn: Strategic and Space Systems (OS)

Deputy Chief of Staff for Research
Development and Acquisition
Department of the Army
Washington, DC 20310
Attn: DAMA-CSS-N

Commander
Harry Diamond Laboratories
Department of the Army
2800 Powder Mill Road
Adelphi, MD 20783
Attn: DELHD-I-TL (Technical Libary)

Director
U.S. Army Ballistic Research Laboratories
Aberdeen Proving Ground, MD 21005
Attn: DRDAR-TSB-S (Technical Library)

Director
U.S. Army Engineering Waterways
Experimental Station
P.O. Box 631
Vicksburg, MS 39180
Attn: J. Strange
N. Flathau
Technical Information Center

Commander
U.S. Army Material and
Mechanics Research Center
Watertown, MA 02172
Attn: DRXMR-TE, R. Shea

Commander
U.S. Army Nuclear and
Chemical Agency
7500 Backlick Road, Bldg. 2073
Springfield, VA 22150
Attn: Library

Commander
David Taylor Naval Ship
Research and Development Center
Bethesda, MD 20084
Attn: Code 174 1740.6
1740.4 L42-3 (Library)
1740.1 11
173 1740.5
1844 172
1770.1 2740

Officer in Charge
Naval Construction Battalion Center
Civil Engineering Laboratory
Port Hueneme, CA 93041
Attn: Code L08A (Library)

Commander
Naval Electronic Systems Command
Washington, DC 20360
Attn: PME 117-21

Commander
Naval Facilities Engineering Command
Washington, DC 20390
Attn: Code 09M22C (Technical Library)

Headquarters
Naval Material Command
Washington, DC 20360
Attn: MAT 08T-22

Commander
Naval Ocean Systems Center
San Diego, CA 92152
Attn: Code 4471 (Technical Library)

Superintendent
Naval Postgraduate School
Monterey, CA 93940
Attn: Code 0142 (Library)
69NE

Commander
Naval Sea Systems Command
Washington, DC 20362
Attn: SEA 08
SEA 322
SEA 09G53 (Library)
SEA 323
SEA 3221

Commanding Officer
Naval Research Laboratory
Washington, DC 20375
Attn: Code 8100
8440
8003
8301
6380
2627 (Technical Library)
8445

Officer in Charge
Naval Surface Weapons Center
White Oak Laboratory
Silver Spring, MD 20910
Attn: Code R14
R13
F31
R10
R15

Commander
Naval Surface Weapons Center
Dahlgren, VA 22448
Attn: Technical Library and
Information Services Branch

Commander
Naval Weapons Center
China Lake, CA 93555
Attn: Code 233 (Technical Library)

Commanding Officer
Naval Weapons Evaluation Facility
Kirtland Air Force Base
Albuquerque, NM 87117
Attn: Code 210
10 (Technical Library)
G. Binns

Commanding Officer
NWSC Crane
Crane, IN 47401
Attn: Code 70553

Officer in Charge
New London Laboratory
Naval Underwater Systems Center
New London, CT 06320
Attn: Code 401, J. Kalinowski
401, J. Patel

Officer in Charge
Newport Laboratory
Naval Underwater Systems Center
Newport, RI 02840
Attn: Code EM
363, P. Paranzino

Office of Naval Research
Arlington, VA 22217
Attn: Code 474, N. Perrone

Office of the Chief of Naval Operations
Washington, DC 20350
Attn: OP 981
OP 982 OP 37
OP 953 OP 604C
OP 981N1 OP 03EG
OP 957E OP 987
OP 951 OP 21

Director
Strategic Systems Project Office
Department of the Navy
Washington, DC 20376
Attn: NSP-272
NSP-43 (Technical Library)

Air Force Institute of Technology
Air University
Wright-Patterson Air Force Base
Dayton, OH 45433
Attn: Library

Air Force Weapons Laboratory, AFSC
Kirtland Air Force Base
Albuquerque, NM 87117
Attn: SUL

Bolt Beranek & Newman, Inc.
Union Station
New London, CT 06320
Attn: R. Haberman

Cambridge Acoustical Associates, Inc.
54 Rindge Avenue Extension
Cambridge, MA 02140
Attn: M. Junger

Columbia University
Department of Civil Engineering
S. W. Mudd Building
New York, NY 10027
Attn: F. DiMaggio

General Dynamics Corporation
Electric Boat Division
Eastern Point Road
Groton, CT 06340
Attn: M. Pakstys

General Electric Co.
816 State Street
P.O. Drawer QQ
Santa Barbara, CA 93102
Attn: DASIAC

Kaman Sciences Corp.
P.O. Box 7463
Colorado Springs, CO 80933
Attn: Library

Merritt Cases, Inc.
P.O. Box 1206
Redlands, CA 92373
Attn: Library

Pacifica Technology
P.O. Box 148
Del Mar, CA 92014
Attn: J. Kent

Patel Enterprises, Inc.
2907 Governors Drive
Huntsville, AL 35805
Attn: M. Patel

Physics Applications, Inc.
828 Charcot Avenue
San Jose, CA 95131
Attn: C. Vincent

SRI International
333 Ravenswood Avenue
Menlo Park, CA 94025
Attn: G. Abrahamson
A. Florence

Tetra Tech, Inc.
630 N. Rosemead Boulevard
Pasadena, CA 91107
Attn: Library (Unclassified Only)
L. Hwang (Unclassified Only)

Weidlinger Associates Consulting
Engineers
110 East 59th Street
New York, NY 10022
Attn: M. Baron

Weidlinger Associates Consulting
Engineers
3000 Sand Hill Road
Menlo Park, CA 94025
Attn: J. Isenberg

SECURITY CLASSIFICATION OF THIS PAGE (When Data Entered)

REPORT DOCUMENTATION PAGE

READ INSTRUCTIONS BEFORE COMPLETING FORM

1. REPORT NUMBER: LMSC-D686495	2. GOVT ACCESSION NO.: AD-A096686
3. RECIPIENT'S CATALOG NUMBER:	
4. TITLE (and Subtitle): DAMAGE CHARACTERISTICS OF AN INFINITE CYLINDRICAL SHELL EXCITED BY A TRANSIENT ACOUSTIC WAVE	5. TYPE OF REPORT & PERIOD COVERED: Final Report for Period 1 July 1979-31 March 1980
	6. PERFORMING ORG. REPORT NUMBER: LMSC-D686495
7. AUTHOR(s): T. L. Geers, C. L. Yen	8. CONTRACT OR GRANT NUMBER(s): N00014-79-C-0619
9. PERFORMING ORGANIZATION NAME AND ADDRESS: Lockheed Palo Alto Research Laboratory, 3251 Hanover Street, Palo Alto, CA 94304	10. PROGRAM ELEMENT, PROJECT, TASK AREA & WORK UNIT NUMBERS: 61153N, RR02303, RR0230301
11. CONTROLLING OFFICE NAME AND ADDRESS: Office of Naval Research, 800 N. Quincy Street, Arlington, VA 22217	12. REPORT DATE: March 1980
	13. NUMBER OF PAGES: 21
14. MONITORING AGENCY NAME & ADDRESS(if different from Controlling Office)	15. SECURITY CLASS. (of this report): UNCLASSIFIED
	15a. DECLASSIFICATION/DOWNGRADING SCHEDULE

16. DISTRIBUTION STATEMENT (of this Report)

Approved for public release; distribution unlimited.

17. DISTRIBUTION STATEMENT (of the abstract entered in Block 20, if different from Report)

18. SUPPLEMENTARY NOTES

19. KEY WORDS (Continue on reverse side if necessary and identify by block number)

Fluid-Structure Interaction
Inelastic Behavior
Transient Shell Response

20. ABSTRACT (Continue on reverse side if necessary and identify by block number)

An analytical/computational technique previously developed for determining the geometrically and constitutively nonlinear response of a submerged, infinite cylindrical shell to a transverse, transient acoustic wave is used to study the damage behavior of the shell. Incident waves of rectangular pressure-profile are considered, nonlinear transient response computations are performed, and damage results are described in terms of iso-damage curves based on extensional set strain. Results generated through the use of the doubly asymptotic appoximation for treatment of the fluid-structure interaction differ

(Reverse Side)

DD FORM 1 JAN 73 1473 EDITION OF 1 NOV 65 IS OBSOLETE

SECURITY CLASSIFICATION OF THIS PAGE (When Data Entered)

20. ABSTRACT

appreciably from their exact counterparts.


DA
FILM